Numerical method for interaction among multi-particle, fluid and arbitrary shape structure

Kensuke Yokoi[1,2]
[1]Mathematics Department, University of California,
Los Angeles CA 90095-1555, USA.
[2]Department of Electronics and Mechanical Engineering,
Chiba University, Chiba, 263-8522, Japan

May 31, 2006

Abstract

We propose a numerical method for handling with interaction among multiple particles, fluid and structure of arbitrary shape. The method is based on the level set method, the discrete element method, the CIP method and the ghost fluid method. In the formulation, the level set method is used to impose fluid boundary condition on structure and particle and to detect collision between particle and structure. Numerical results show that this proposed method can robustly simulate the interactions.

keywords: particle-fluid-structure interaction, level set method, discrete element method, CIP method

1 Introduction

Particle simulations have been widely used in various fields in science and engineering. Simulating interaction among particle, fluid and structure is important for practical applications such as drug delivery in blood vessel, and control of sand erosion in desert, sea and river. In the paper, we propose a numerical method based on Navier-Stokes equations and a regular Cartesian grid to deal with these phenomena.

To simulate interaction among particles, the discrete element method (DEM) [1, 2, 3] has been widely used. In DEM, particles overlap during collision and the dynamics is defined though the force acting on the collision

particles. DEM can deal with many-body collision and can sustain contact between particles. The present method is based on DEM for collision detection. Although we just use DEM to compute interaction among particles, for computing interaction between particle and structure, we couple DEM with the level set method [4].

In the present method, arbitrary shape structure is represented by the zero-level set of level set function. Although the level set method [5, 7, 8, 6] is an interface capturing method, it has been used in various fields such as computational fluid dynamics and solid dynamics, image processing, and material science. The level set method is convenient to compute the interaction among particles and structure, and to impose fluid boundary condition on the structure. Level set functions for particles are also constructed, based on the position of particle center, for computing interaction between particles and fluid, and fluid boundary condition. The important features of the level set method are that the unit normal for the interface and the distance from the interface are well defined. These characteristics play an important role in calculating fluid boundary condition on the structure and particles by coupling with the ghost fluid method [9, 10, 11], and collision detection between particles and structure.

Numerical simulations of fluid structure interaction have been done by many researchers [12, 13, 14, 11]. The immersed boundary method [12] may be used most widely. Some numerical methods for fluid-particle interaction have been proposed [15, 16, 17]. In this paper, we used a method based on the level set method and a volume force formulation [13, 14] to calculate the force from fluid to particle.

In this paper, we propose a method for handling particle-fluid-structure interaction based on the level set method systematically. The numerical method and the validation are discussed in section 2 and 3, respectively. After the simulation results and discussions in section 4, a short summary comes in section 5.

2 Numerical method

2.1 Governing equations

We use the following governing equations for fluid

$$\nabla \cdot \mathbf{u} = 0, \tag{1}$$

$$\frac{\partial \mathbf{u}}{\partial t} + (\mathbf{u} \cdot \nabla)\mathbf{u} = -\frac{\nabla p}{\rho} + \frac{\nabla \cdot \tau}{\rho} + \frac{\mathbf{f}}{\rho}, \tag{2}$$

where $\mathbf{u}$ is the velocity, p the pressure, ρ the density, τ the viscous stress tensor and $\mathbf{f}$ the body force. These equations are solved based on the

fractional step method [18] with the CIP method [19, 20] of an advection equation solver. See [19, 20] for more details.

Equations for translational and rotational motion for a spherical particle are

$$m\frac{d^2\mathbf{r}}{dt^2} = \mathbf{F}_{particle} + \mathbf{F}_{structure} + \mathbf{F}_{fluid}, \tag{3}$$

and

$$\mathbf{I}\frac{d\omega}{dt} = \mathbf{T}_{particle} + \mathbf{T}_{structure} + \mathbf{T}_{fluid}, \tag{4}$$

where $\mathbf{r}$ is the position of particle center, m is the mass of particle. $\mathbf{F}_{particle}$, $\mathbf{F}_{structure}$ and $\mathbf{F}_{fluid}$ are forces from other particles, structure and fluid, respectively. ω is the angular velocity. $\mathbf{T}_{particle}$, $\mathbf{T}_{structure}$ and $\mathbf{T}_{fluid}$ are the torque due to forces from other particles, structure and fluid, respectively. $\mathbf{I}$ is the moment of inertia.

2.2 Level set method

The level set method expresses the surface of an $N-1$ dimension as a zero level (or contour) of an N-dimensional level set function ψ. The signed distance function

$$\begin{aligned} \psi &= 0 \quad \text{at the interface} \\ |\nabla\psi| &= 1 \quad \text{for the whole region} \end{aligned} \tag{5}$$

is used as the level set function as shown in Fig. 1. In the paper, the

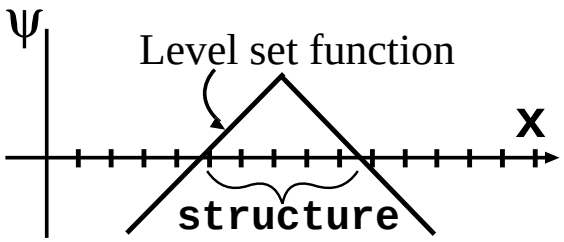

Figure 1: Schematic figure of a level set function in the one dimensional case.

level set method is used on a regular Cartesian fixed grid. Although the Cartesian fixed grid is used, the level set formulation can express subgrid information and complex geometries as shown in Fig. 1 and Fig. 2. An advantage of the level set method is that the unit normal is always well

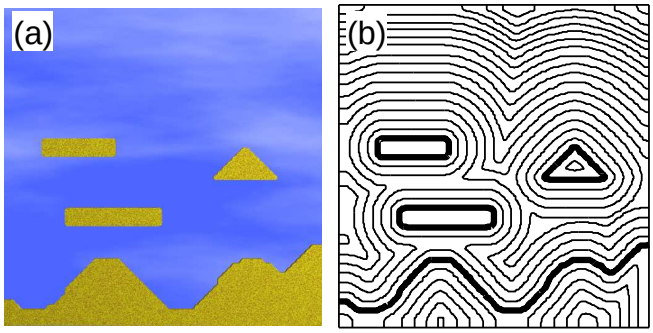

Figure 2: An example of a level set function in the two dimensional case. (a) shows the shape of structures. (b) shows the contour lines of the level set function for the structure. The thick and thin lines represent the zero level set and the contour lines of the level set function. A 70×70 Cartesian grid is used.

defined from the level set function

$$\mathbf{n}_{ls} = \frac{\nabla \psi}{|\nabla \psi|}. \tag{6}$$

The unit normal is useful for computing interaction between particles and structures by using the distance function.

To construct the level set function for structures, we can use methods found in [21, 7, 22, 23, 24] such as the Fast Marching method for solving the Eikonal equation

$$|\nabla \psi| = 1. \tag{7}$$

The density (color) function ϕ, which is used to define the physical properties of different materials, can be generated as a smoothed Heaviside function

$$\phi = H_\alpha(\psi), \tag{8}$$

for instance

$$H_\alpha(\psi) = \begin{cases} 0 & \text{if} \quad \psi < -\alpha \\ \frac{1}{2}[1 + \frac{\psi}{\alpha} + \frac{1}{\pi} sin(\frac{\pi \psi}{\alpha})] & \text{if} \quad |\psi| \leq \alpha \\ 1 & \text{if} \quad \psi > \alpha\,, \end{cases} \tag{9}$$

where 2α represents the distance of the transition region between the fluid region and the solid region. In this paper, we used $2\alpha = 1$.

2.3 Particle-particle interaction (DEM)

Contact forces between spherical particles are modelled by a linear spring, a dashpot and a friction slider [1]. The normal interaction is expressed by a linear spring and a dashpot (Fig.3(a)), and the tangential interaction is expressed by a linear spring, a dashpot and a friction slider (Fig.3(b)).

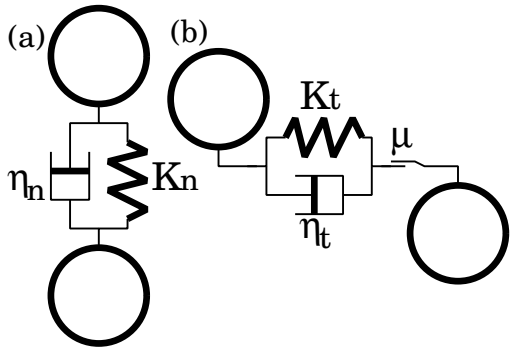

Figure 3: Schematic figure of the discrete element method. K, η and ν refer to the linear spring, the dash pot and the slider, respectively

We consider two disks i and j of diameters d_i and d_j, with masses m_i and m_j, particle centers $\mathbf{r_i}$ and $\mathbf{r_j}$, velocities at mass center $\mathbf{c}_i$ and $\mathbf{c}_j$, and the angular velocities ω_i and ω_j. The contact forces are calculated in contact, namely,

$$\Delta \equiv \frac{d_i + d_j}{2} - |r_{i,j}| > 0, \tag{10}$$

where $\mathbf{r}_{i,j} \equiv \mathbf{r}_i - \mathbf{r}_j$ The normal component of the contact force $F_n^{i,j}$ due to the particle j acting on the particle i is

$$F_n^{i,j} = 2Mk_n\Delta - 2M\eta_n v_n, \tag{11}$$

with

$$v_n = (\mathbf{c}_i - \mathbf{c}_j) \cdot \mathbf{n}, \tag{12}$$

$$\mathbf{n} = \frac{\mathbf{r}_{i,j}}{|\mathbf{r}_{i,j}|}, \quad \mathbf{r}_{i,j} = \mathbf{r}_i - \mathbf{r}_j \tag{13}$$

where M is the reduced mass ($M = m_i m_j/(m_i + m_j)$), k_n the spring constant, η_n the normal damping coefficient and v_n the normal component of the relative velocity, $\mathbf{n}$ the unit normal. The tangential component of the contact force $F_s^{i,j}$ is

$$F_s^{i,j} = min(|h_s^{i,j}|, \mu|F_n^{i,j}|)sgn(h_s^{i,j}), \tag{14}$$

with

$$h_s^{i,j} = -2Mk_s u_s - 2M\eta_s v_s, \tag{15}$$

$$u_s = \int_{t_0}^{t} v_s dt, \tag{16}$$

$$v_s = (\mathbf{c}_i - \mathbf{c}_j) \cdot \mathbf{s} + (\frac{d_i}{2}\omega_i + \frac{d_j}{2}\omega_j), \tag{17}$$

where μ is the Coulomb friction coefficient for slider, k_s the tangential spring constant, u_s the tangential displacement, t_0 the time at the impact, η_s the tangential damping parameter, v_s the tangential velocity, $\mathbf{s}$ the unit tangential vector. $\mathbf{F}_{particle,i}$ and $\mathbf{T}_{particle,i}$ are calculated as follows

$$\mathbf{F}_{particle,i} = \Sigma_j (F_n^{i,j} + F_s^{i,j}), \tag{18}$$

$$\mathbf{T}_{particle,i} = \frac{d_i}{2}\Sigma_j (\mathbf{n} \times F_s^{i,j}). \tag{19}$$

As the time step, $\Delta t < 2\sqrt{\frac{2M}{k_n}}$ introduced in [1] is used.

2.4 Structure-particle interaction (level set method)

The interaction between the structures expressed by the level set function and particles are computed based on DEM. The structure is represented by the zero-level set of the level set function This means the distance from the structure and the normal vector for the structure are assigned on each grid point. Here, the normal vector is calculated as the gradient of the level set function. To compute collision between a structure and a particle, the distance between the particle and the structure, and the normal direction for the structure are required. These informations can be obtained by interpolating the level set function at the center of the particle. Therefore, DEM is slightly modified by using the level set function ψ and the $\mathbf{n}_{ls}$ of (6). The procedures of DEM are replaced as follows:

$$(10) \Rightarrow \quad \Delta \equiv \frac{d_i}{2} - |\psi| > 0, \tag{20}$$

$$(11) \Rightarrow \quad F_n^{i,ls} = k_n \Delta - \eta_n v_n, \tag{21}$$

$$(12) \Rightarrow \quad v_n = \mathbf{c}_i \cdot \mathbf{n}_{ls}, \tag{22}$$

$$(13) \Rightarrow \quad \mathbf{n}_{ls} = \mp \frac{\nabla \psi}{|\nabla \psi|}, \tag{23}$$

$$(14) \Rightarrow \quad F_s^{i,ls} = min(|h_s^{i,ls}|, \mu |F_n^{i,ls}|) sgn(h_s^{i,ls}), \tag{24}$$

$$(15) \Rightarrow \quad h_s^{i,ls} = -k_s u_s - \eta_s v_s, \tag{25}$$

$$(16) \Rightarrow \quad u_s = \int_{t_0}^{t} v_s dt, \tag{26}$$

$$(17) \Rightarrow \quad v_s = \mathbf{c}_i \cdot \mathbf{s}_{ls} + \frac{d_i}{2}\omega_i, \tag{27}$$

here ψ_i is ψ at the position of particle center. ψ_i is estimated by using an interpolation. The bilinear interpolation is used in this paper. In (23), "+" sign is used for $\psi_{structure} > 0$ and "−" sign is used for $\psi_{structure} < 0$. $\mathbf{F}_{structure,i}$ and $\mathbf{T}_{structure,i}$ are calculated as follows

$$\mathbf{F}_{structure,i} = \Sigma_j (F_n^{i,j} + F_s^{i,j}), \tag{28}$$

$$\mathbf{T}_{structure,i} = \frac{d_i}{2}\Sigma_j (\mathbf{n} \times F_s^{i,j}). \tag{29}$$

As the time step for the interaction between a particle and level set function, $\Delta t < 2\sqrt{\frac{m_i}{k_n}}$ is used.

2.5 Particles-fluid interaction

The force and the torque from fluid to moving solid object are determined by the equations

$$\mathbf{F}_{fluid} = \int \rho \frac{d\mathbf{u}}{dt}\phi_i dV \tag{30}$$

and

$$\mathbf{T}_{fluid} = \int (\mathbf{r_1} \times \rho \frac{d\mathbf{u}}{dt})\phi_i dV, \tag{31}$$

ϕ_i is the color function of each particle and $\mathbf{r_1}$ is the position vector from the mass center. See [13, 14] for more details. The color function is calculated from the level set function by using a smoothed Heaviside function (9). The level set function for each particle is calculated as follow:

$$\psi_i = \sqrt{(x - x_i)^2 + (y - y_i)^2} - \frac{d_i}{2}. \tag{32}$$

2.6 Fluid boundary condition

To impose a boundary condition on a solid object, we use the ghost fluid method. In this method, imaginary cells called ghost cells are placed within a few grids from the interface in the solid region. The variables of fluid near the interface are extrapolated into the ghost cells to satisfy the boundary condition on the solid surface.

The velocity u_{ghost} on the ghost cells is estimated by a linear extrapolation using the level set function as follows

$$\mathbf{u}_{ghost} = \frac{\psi_{ghost}}{\psi_{fluid}}\mathbf{u}_{fluid} + (1 - \frac{\psi_{ghost}}{\psi_{fluid}})\mathbf{u}_{surf}, \tag{33}$$

here, u_{fluid} and u_{surf} are the velocity near the solid in the fluid and the velocity of the solid surface, respectively as shown in Fig. 4. ψ_{ghost} is the level set function at the position where $\mathbf{u}_{ghost}$ is defined. From the definition of (33), the order of accuracy of the velocity boundary condition is first order. In this study, we used $\psi_{fluid} = \mp\Delta x$, where "$-$" sign is used

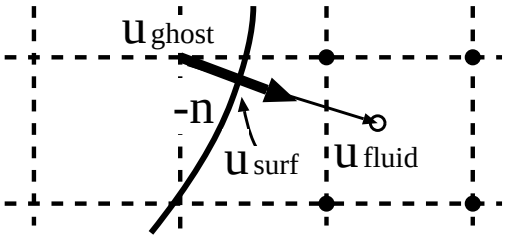

Figure 4: Schematic figure of the ghost fluid method. The curve represents the solid interface. This is for $\psi_{ghost} > 0$. If $\psi_{ghost} < 0$, replace $-\mathbf{n}$ to $\mathbf{n}$.

for $\psi_{fluid} < 0$ and "$+$" is used for $\psi_{fluid} > 0$. $\mathbf{u}_{fluid}$ is derived by solving the following equation

$$\frac{\partial \mathbf{u}}{\partial t_g} \pm \mathbf{n} \cdot \nabla \mathbf{u} = 0 \tag{34}$$

here, "$+$" sign is for $\psi_{ghost} > 0$, "$-$" is for $\psi_{ghost} < 0$, and t_g is an artificial time, in this case $\Delta t_g = |\psi_{ghost}| + |\psi_{fluid}|$.

We use a semi-Lagrangian approach to solve (34) because $\mathbf{n}\Delta t_g$ is usually more than Δx (i.e., CFL number > 1) as shown in Fig. 4. We use the semi-Lagrangian scheme using bi-linear interpolation. In the semi-Lagrangian formulation, the interpolation function is constructed using the grid points surrounding the position where $\mathbf{u}_{fluid}$ is defined, marked by the black circles in Fig. 4. We use the following interpolation function

$$F(x,y) = a_{11}XY + f_x X + f_y Y + f_{i',j'}, \tag{35}$$

$$X = x - x_{i',j'}, Y = y - y_{i',j'}, \tag{36}$$

$$f_x = \frac{f_{iup',j'} - f_{i',j'}}{\Delta x}, f_y = \frac{f_{i',jup'} - f_{i',j'}}{\Delta y}. \tag{37}$$

$$a_{11} = \frac{f_{iup',jup'} - f_{i',j'}}{\Delta x \Delta y} - \frac{f_x \Delta x + f_y \Delta y}{\Delta x \Delta y}, \tag{38}$$

here $i' = i + int(-n_x \Delta t_g / |\Delta x|)$, $iup' = i' + sign(-n_x \Delta t_g)$, $\Delta x = x_{iup',j'} - x_{i',j'}$, $int(a)$ means the integer part of a. $\mathbf{u}_{fluid}$ can be computed from

$F(x_{i,j}-n_x\Delta t_g, y_{i,j}-n_y\Delta t_g)$ or $F(x_{i',j'}-\mathrm{mod}(n_x\Delta t_g/|\Delta x|), y_{i',j'}-\mathrm{mod}(n_y\Delta t_g/|\Delta y|))$ where $mod(a/b)$ means the reminder of a/b.

The pressure boundary condition is computed by solving the pressure Poisson equation over all the computational domain including the solid region.

3 validation

To certify the present method for particle-structure interaction, we carried out a simple test problem. Fig. 5 shows the configuration. The slope is

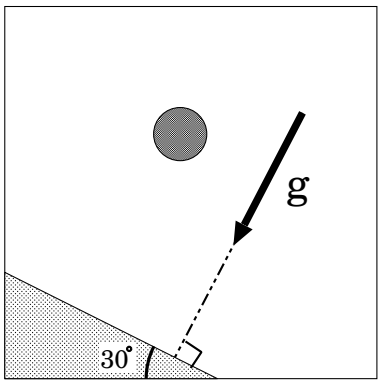

Figure 5: Schematic figure of a test problem.

represented by the level set function on a Cartesian fixed grid of 50×50. The direction of gravity is perpendicular to the slope. In this test problem, damping and rotation of the particle are not taken into account. In this configuration, if the particle is released with the velocity= 0 from height h for the slope, the particle must return to the same position at $t = 2\sqrt{2h/g}$. The numerical result compared with the exact solution is shown in Fig. 6. Table 1 displays the errors at $t = 2, 4, 6, 8$[s]. Error_1 and error_2 are defined as error_1=|(numerical result)-(exact solution)| and error_2=error_1/h.

To check the validity of this method for fluid-structure interaction, we used it to solving two-dimensional Poiseuille and Couette flow problems. The theoretical solution of Poiseuille flow is $u_x = \dfrac{a^2}{2\mu}(-\dfrac{dp}{dy})(1-\dfrac{x^2}{a^2})$, where a is a wall width. Fig. 7 shows a comparison between the numerical results and theoretical solutions for various wall widths. The velocity profiles agree well with the analytical solutions even in a small number of grids.

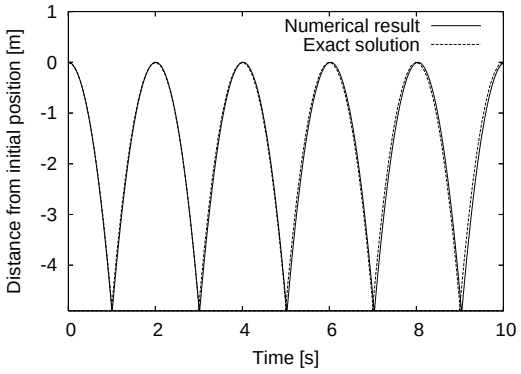

Figure 6: Time evolution of the height of particle from the slope. The solid line and the dotted line represent the numerical result and exact solution, respectively. Five cycles are plotted. $k_n = 5 \times 10^7$ is used.

Table 1: Error of this algorithm.

Time(s)	$Error_1$	$Error_2$
2	2.98×10^{-4}	6.08×10^{-5}
4	1.25×10^{-3}	2.55×10^{-4}
6	2.87×10^{-3}	5.86×10^{-4}
8	5.14×10^{-3}	1.05×10^{-3}
10	8.08×10^{-3}	1.65×10^{-3}

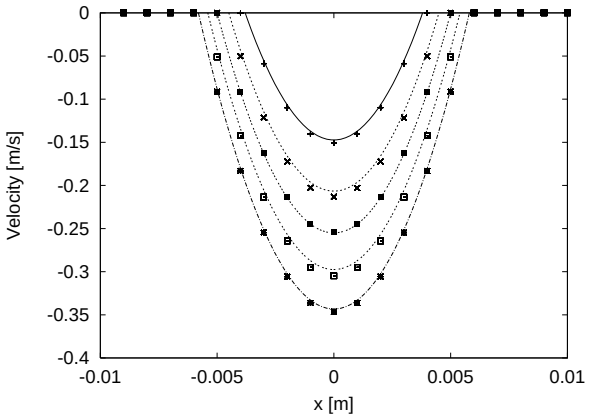

Figure 7: Comparison between the numerical and theoretical velocity profiles for various wall widths. The dots and lines represent the numerical and theoretical solutions respectively. The viscosity coefficient $\mu = 4.9 \times 10^{-3}$ Pa·s, $dp/dy = 100$ Pa/m and $\Delta x = \Delta y = 1$mm are used.

To validate (33) for a moving wall and the influence of a rectangular grid for a circular shape, the method was applied for a Couette flow problem. The configuration is shown in Fig. 8. Liquid is put in a cylinder

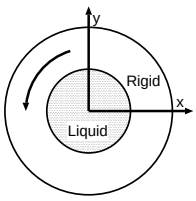

Figure 8: Configuration of a Couette flow.

and the cylinder is rotated at a constant angular velocity ω_{cyl}. Then the theoretical solution of the velocity profile is $v(r) = \omega_{cyl} r_{cyl}$, here r_{cyl} is the radius of the cylinder. In this simulation, the shape of the cylinder is imposed through the level set function analytically $\psi(x, y) = \sqrt{x^2 + y^2} - r_{cyl}$. Therefore, the shape is represented well in the grid system. The rotation of the rigid body is expressed through $\mathbf{u}_{surf}$ on the ghost cells, $u_{surf,x} = -\omega_{cyl} y_{cyl} = -\omega_{cyl} r_{cyl} n_y$ and $u_{surf,y} = \omega_{cyl} x_{cyl} = \omega_{cyl} r_{cyl} n_x$ here, $\psi_{ghost} > 0$. If $\psi_{ghost} < 0$, replace n_x and n_y with $-n_x$ and $-n_y$. Fig.

Table 2: Results of the numerical convergence studies. $Error_p$ and $Error_c$ are the errors for the velocity at $x = 0$ in the Poiseuille flow problem and at $radius = 0.4$ mm in the Cuette flow problem, respectively.

Grid spacing	1mm	0.5mm	0.25mm
$Error_p$	2.16×10^{-2}	1.03×10^{-2}	4.67×10^{-3}
$Error_c$	3.75×10^{-2}	2.00×10^{-2}	1.23×10^{-2}

9 shows a comparison between the numerical and theoretical solutions. The dots show the y velocity component on the x axis. The results show

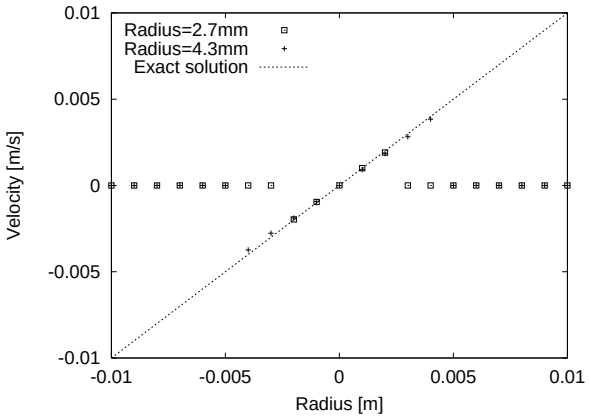

Figure 9: The dots and lines represent the numerical and theoretical solutions respectively. As the radii of the cylinder, 2.7 and 4.3 mm are used. The angular velocity $\omega_{cyl} = 1.0$.

that (33) is appropriate and that the method is appropriate for treating a circular shape in a Cartesian grid.

Numerical convergence studies are performed for the Poiseuille problem of the wall width 3.8 mm and the Couette problem of the cylinder radius 4.3 mm. The error is defined as $Error = \dfrac{|u_{sim} - u_{exact}|}{|u_{exact}|}$, here u_{exact} and u_{sim} are the velocity of the exact solution and the simulation respectively. These errors are declined linearly as shown in Table 2. The results show that the method has first order accuracy.

4 Numerical result

4.1 Interaction among particles, air and liquid

We carried out numerical simulation in which the particles interact with liquid interface under gravity. As a set of parameters, we use $k_n = 5 \times 10^7$, $\eta_n = 2\sqrt{k_n}$, $k_s = 0.2k_n$, $\eta_s = \eta_n$ and $\mu = 0.5$ for particles, the density $\rho_{liquid} = 1000$ kg/m^3, $\rho_{gas} = 1.25$ kg/m^3 the kinematic viscosity $\mu_{liquid} = 1.0 \times 10^{-3}$ kg s/m^2, $\mu_{gas} = 1.8 \times 10^{-5}$ kg s/m^2. A 100×100 grid is used for fluid calculation and the level set function. Fig. 10 shows the numerical results when 50 particles interact with gas and liquid. The liquid

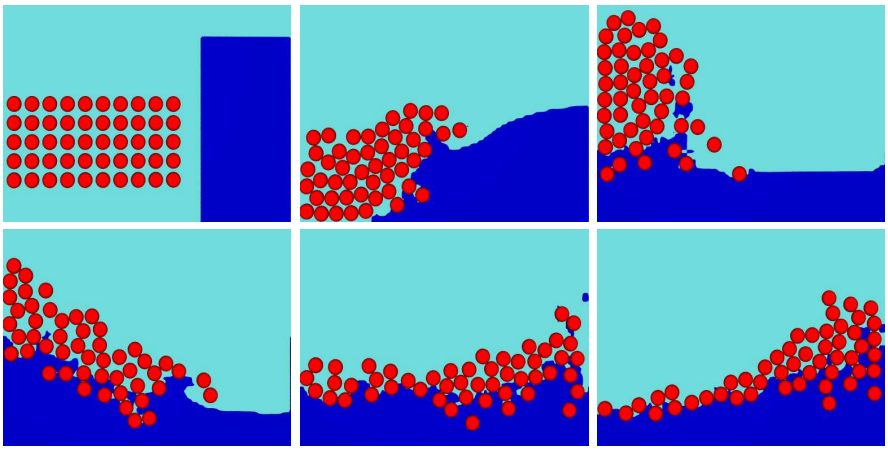

Figure 10: Time series of the numerical simulation of dam break with the 50 particles, the air and the structures. The density ratio of air:particle:liquid is 1.25:500:1000.

accelerated by the gravity hit those particles from right to left. The results show that the method is robust.

4.2 Interaction among particles, fluid and complex structures

Fig. 11 represents the result of interaction among particles, air and complex structure. Fig. 12 is the vector field. We can see that the air goes up among the particles as shown in Fig. 11 and Fig. 12 at t=1.8. This is because the air under the particles must blow up instead of these particles if the particles fall in incompressive fluid as shown in Fig. 11. Complex vortex structure are formed as shown in Fig. 12. As a comparison, we display the

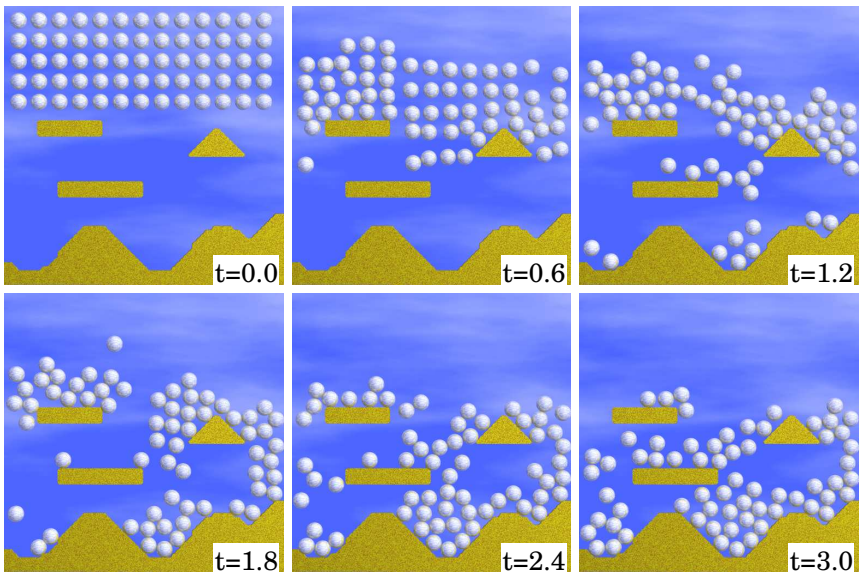

Figure 11: Time series of the numerical simulation of interaction among the 65 particles, the air and the structures. The density ratio of air:particle is 1.25:500.

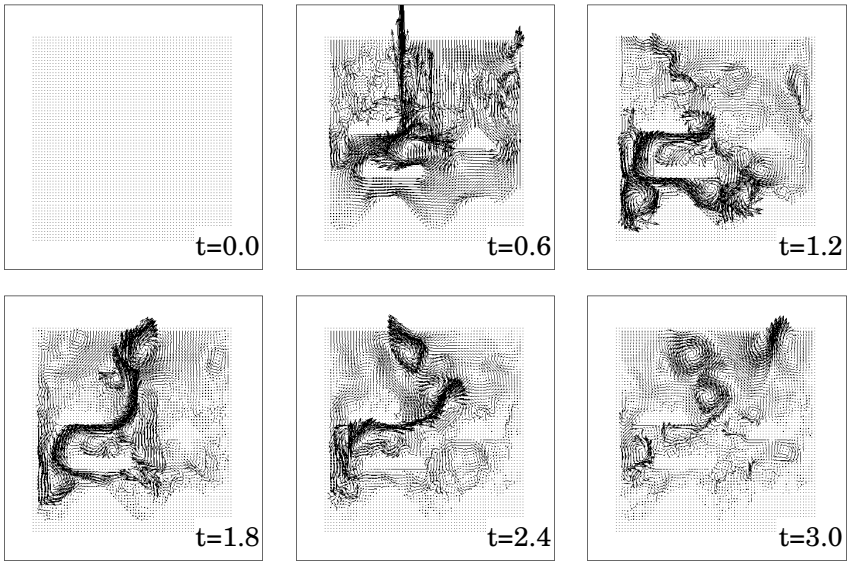

Figure 12: Time series of the velocity fields of Fig. 11.

result of the case without fluid in Fig. 13. In the simulation no blowing up is observed.

Fig. 14 shows the numerical result that 7 particles flow as interacting with fluid in a tube of complex geometry. The flow is from left to right. As an inlet boundary condition, we used the velocity profile of Poiseuille flow. The method can deal with the interaction among particles, fluid and complex structure robustly.

5 summary

We have proposed a numerical method based on the level set method, CIP method and the ghost fluid method for capturing a moving solid object that interacts with fluid in a Cartesian fixed grid. The validity of the method has been shown by the test problems of Couette and Poiseuille flows. The results of simulation of a rigid falling into the liquid show that the method precisely captures a moving solid object and liquid surface in a small number of grids and that the model is robust.

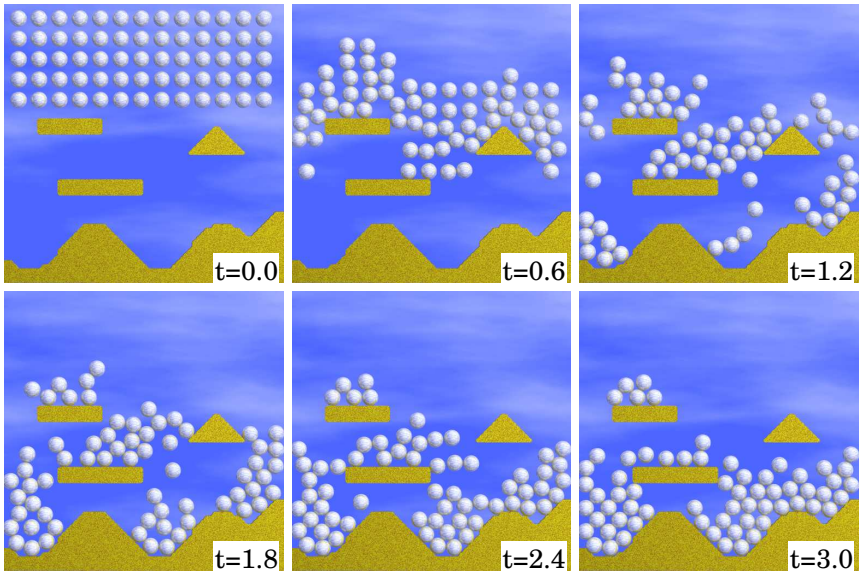

Figure 13: Time series of the numerical simulation of interaction between the 65 particles and structure without air.

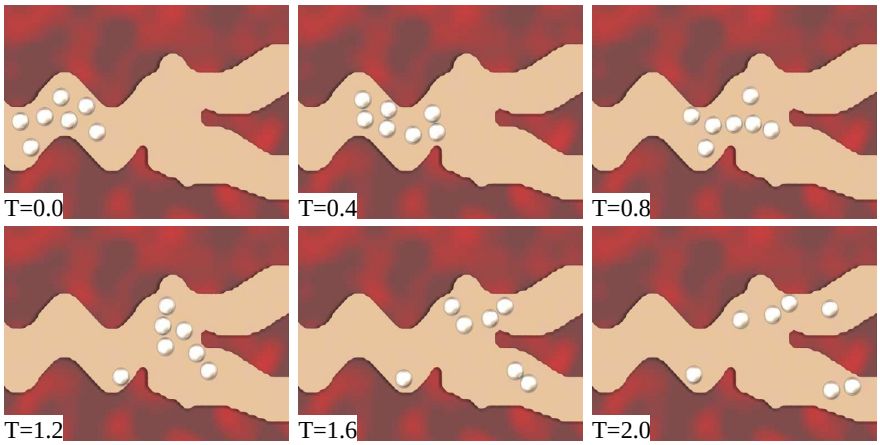

Figure 14: Time series of the numerical simulation of interaction among the 7 particles, fluid and structure. The density ratio of fluid:particle is 1.25:500. The Reynolds number at the inlet boundary is 200.

6 Acknowledgements

We would like to thank Shingyu Leung, Stanley Osher and Hao Liu for their useful discussions and comments. This work was supported in part by a Grant-in-Aid for JSPS fellow (17-4063) of Japan Society for the Promotion of Science. Numerical computations in this work was partially carried out at the Yukawa Institute for Theoretical Physics, Kyoto University.

References

[1] P.A. Cundall O.D.L. Strack, A discrete numerical model for granular assemblies, Geotechnique, **29** 47 (1979).

[2] C.S. Campbell, Rapid granular flow, Annual Review of Fluid Mechanics, **22** 57 (1990).

[3] G. Mustoe (ed.), Engineering Computation **9**(2) Special Issue (1992).

[4] K. Yokoi, Numerical method for interaction between multiparticle and complex structures , Phys. Rev. E, **72**, 046713 (2005).

[5] S. Osher and J.A. Sethian, Front propagating with curvature-dependent speed: Algorithms based on Hamilton-Jacobi formulation, J. Comput. Phys. **79**, 12 (1988).

[6] M. Sussman, P. Smereka and S. Osher, J. Comput. Phys. **114**, 146 (1994).

[7] J.A. Sethian, Level Set Methods and Fast Marching Methods, Cambridge University Press (1999).

[8] S. Osher and R. Fedkiw, Level Set Methods and Dynamics Implicit Surface, Applied Mathematical Sciences 153, Springer (2003).

[9] R. Fedkiw et al., J. Comput. Phys. **152**, 457 (1999).

[10] M. Watanabe, R. Kikinis and C.F. Westin, Lecture Notes in Computer Science 2489, Springer, 405 (2002).

[11] K. Yokoi, Numerical method for moving solid object in flows, Phys. Rev. E, **67**, 045701(R) (2003).

[12] C.S. Peskin, J. Comput. Phys. **25**, 220 (1977).

[13] F. Xiao et al., Comput. Phys. Commun. **102** 147 (1997).

[14] F. Xiao, J. Comput. Phys. **155**, 348 (1999).

[15] T. Tanaka, T. Kawaguchi and Y. Tsuji, Discrete Particle Simulation of Flow Patterns in Two-Dimensional Gas Fluidized Beds Int. J. Modern Physics B, **7**, 1889 (1993).

[16] A.J.C. Ladd, Numerical simulations od particulate flow suspensions via a discretized Boltzmann equation. Part II: Numerical results, J. Fluid Mech, **271**, 311 (1994).

[17] Z.G. Feng, E.E. Michaelides, Proteus: a direct forcing method in the simulation of particulate flows, J. Comput. Phys. **202**, 20 (2005).

[18] J. Kim and P. Moin, Applications of a fractional step method to incompressible Navier-Stokes equations, J. Comput. Phys. **59**, 308 (1985).

[19] T. Yabe et al, Comput. Phys. Commun. **66** 233 (1991).

[20] T. Yabe, F. Xiao and T. Utsumi, J. Comput. Phys. **169**, 2 (2001).

[21] D. Adalsteinsson and J.A. Sethian, The Fast Construction of Extension Velocities in Level Set Methods, J. Comput. Phys. **148**, 2 (1999).

[22] Y.R. Tsai, Rapid and accurate computation of the distance function using grids, J. Comput. Phys. **178** 175 (2001).

[23] K. Yokoi, Numerical method for complex moving boundary problems in a Cartesian fixed grid, Phys. Rev. E **65** 055701(R) (2002).

[24] H.K. Zhao, Fast Sweeping Method for Eikonal Equations, Mathematics of Computation, **74** 603 (2005).